

Design of Human Machine Interface through vision-based low-cost Hand Gesture Recognition system based on deep CNN

Abir Sen · Tapas Kumar Mishra · Ratnakar Dash

Received: date / Accepted: date

Abstract In this work, a real-time hand gesture recognition system based human-computer interface (HCI) is presented. The system consists of six stages: (1) hand detection, (2) gesture segmentation, (3) use of six pre-trained CNN models by using the transfer-learning method, (4) building an interactive human-machine interface, (5) development of a gesture-controlled virtual mouse, (6) use of Kalman filter to estimate the hand position, based on that the smoothness of the motion of pointer is improved. Six pre-trained convolutional neural network (CNN) models (VGG16, VGG19, ResNet50, ResNet101, Inception-V1, and MobileNet-V1) have been used to classify hand gesture images. Three multi-class datasets (two publicly and one custom) have been used to evaluate the model performances. Considering the models' performances, it has been observed that Inception-V1 has significantly shown a better classification performance compared to the other five pre-trained models in terms of accuracy, precision, recall, and F-score values. The gesture recognition system is expanded and used to control multimedia applications (like VLC player, audio player, file management, playing 2D Super-Mario-Bros game, etc.) with different customized gesture commands in real-time scenarios. The average speed of this system has reached 35 fps (frame per seconds), which meets the requirements for the real-time scenario.

Keywords Deep Learning · Hand Gesture Recognition · segmentation · Kalman filter · Human machine Interface · Transfer Learning · virtual mouse

1 Introduction

HCI has become a part of our daily life, such as for entertainment purposes or for getting in touch with the assistive interface. With the growth of computer vision, hand gesture recognition has become a trendy field for interaction between man and machine without physically touching any devices. Imagine a scenario such as smart home automation, where a user uses hand gestures to control devices like TV, music player control, wifi turn off/on, light on/off, and various applications. Another scenario is desktop application controls using hand gestures like VLC player control, audio player control, or 2D-game controls and the development of gesture-controlled virtual mouse and keyboard. So in both cases, users can control applications without physically contacting them, which is very beneficial for physically impaired and older people. There are two types of hand gesture recognition: (1) wearable gloves based [1, 2], and (2) vision-based [3, 4]. The disadvantage of the first method is that it is expensive and requires wearing on hand to recognize gestures, and is also unstable in some environments. The second method is based on image processing, where the pipeline of this methodology is followed as: capturing an image using the webcam, segmentation, feature extractions, and classifications of gestures. But challenges occur during the development of a robust hand-gesture recognition system. Though the performance has been enhanced by using advanced depth-sensing cameras like Microsoft Kinect or Intel Real-Sense, they are relatively costly, so it is still an issue. The second challenge dealt by this project is to build a robust human-machine interface with gesture commands in real-time scenario. The third issue resolved by our work is the implementation of the gesture-controlled virtual mouse in real-time and the

movement of the mouse cursor stably and smoothly. We know that our hand is not always stable for controlling the mouse cursor's movement, especially while changing the gestures to understand different commands. So to resolve these issues, first, we have proposed a vision-based hand gesture recognition system by using CNN models, followed by extending our work to develop a real-time gesture-controlled human-machine interface. To make our system more convenient and user-friendly, we have also developed a virtual mouse with the help of gesture commands. The significant contributions of this article are summarized as follows:

- I. A low-cost vision-based hand gesture recognition system has been illustrated using six pre-trained CNN models with a transfer-learning approach. We have also compared the performance among all the CNN models and the best CNN model has been selected for the real-time inference task.
- II. An interactive human-machine interface using customized hand-gesture commands has been built to control different applications in real-time.
- III. Different events of a physical mouse have been triggered with customized hand gesture commands to build a virtual mouse to make the HCI interface more convenient.
- IV. The Kalman filter has been employed to estimate and update the mouse cursor's position to enhance the smoothness of the cursor's motion and prevent jumping of the cursor on the whole screen from one point to another.

The remainder of this manuscript is structured as follows. In Section 2, literature works related to different hand gesture recognition are illustrated. The proposed methodology is discussed in Section 3. Section 4 deals with experimental details, dataset description, comparative analysis, and the details of the gesture-controlled human-machine interface followed by real-time performance analysis. Section 5 describes the discussion portion. Finally, Section 6 includes the summary of the conclusion and future works.

2 Literature survey

In the past few years, with the rapid growth of computer vision, hand gesture recognition has facilitated the field of human-machine interaction. The computer vision researchers mainly use the web camera and hand gestures as inputs to the gesture recognition systems. But while building a low-cost human-machine interface in real-time, some challenges occur, such as gesture detection by background removal, segmentation, and classifying gesture images in the presence of messy back-

ground. So the classification of gestures is crucial for developing any HCI interface. Various state-of-art works for hand gesture recognition were introduced in the last decade. Some used classification techniques are artificial neural network (ANN) algorithms, Hidden Markov model (HMM), or support vector machine (SVM). For instance, Mantecon et al. [5] proposed a hand gesture recognition system using infrared images captured by Leap motion controller device that produces image descriptors without using any segmentation phase. Next, the descriptors were dimensionally reduced and fed into SVM for final classification. Huang et al. [6] developed a novel hand gesture recognition system by using the Gabor filter for feature extraction tasks and SVM for the classification of hand gesture images. Singha et al. [7] developed a dynamic gesture recognition system in the presence of cluttered background. Their proposed scheme consists of three stages: (1) hand portion detection by three-frame difference and skin-filter technique; (2) feature extraction; (3) feeding the features into ANN, SVM, and KNN classifiers, followed by combining these models to produce a new fusion model for final classification. In [8], after collecting the gesture images from the web camera, skin color segmentation was done to separate the hand region from image sequences. HMM was employed on hand feature vectors to classify complex hand gestures. So in various cases, the pipeline of a vision-based hand gesture recognition system is limited to detection, segmentation, and classification.

But recently, with the rapid growth of computer vision and deep learning, the CNN model has become a popular choice for features extraction and classification tasks. Recent research shows that gesture classification with a deep learning algorithm like CNN has produced better results than earlier proposed schemes. For instance, Yingxin et al. [9] developed a hand gesture recognition system, where the canny edge detection technique was employed for pre-processing and CNN for both feature extraction and classification task. Oyeade et al. [10] presented a vision-based hand gesture recognition for recognizing American Sign language. Their proposed scheme has two stages: (1) segmentation of gesture portion after applying binary thresholding and (2) using CNN architecture to predict the final class. In [11], the authors developed a hand gesture recognition system based on CNN. Later deep convolution generative adversarial networks (DCGAN) was used to avoid the overfitting problem. In [12], the experiment was carried out on publicly available datasets (NUS and American finger-spelling dataset). Here CNN was employed for classifying the static gesture images. Recently, Sen et al. [13] developed a hand gesture recognition system,

which had three stages; (1) gesture detection by binary thresholding, (2) segmentation of gesture portion, (3) training of three custom CNN classifiers in parallel, followed by calculating the output scores of these models to build the ensemble model for final prediction.

To build the HCI interface, a gesture-controlled virtual mouse is necessary that eliminates the physical device dependency. Some literature studies have shown some fruitful results regarding the performance of the gesture-controlled virtual mouse. For example, In [14], Shibly et al. published a paper titled ‘Design and Development of Hand Gesture Based Virtual Mouse’, where the authors developed a gesture-controlled virtual mouse by using web-camera captured frames processing and color detection method for gesture portion detection. In the article titled ‘Design of hand gesture recognition system for human-computer interaction’ [15], the authors proposed a low-cost gesture recognition system in a real-time scenario, which has three stages; (1) skin segmentation, (2) moving gesture detection by motion-based background separation, (3) separate of arm portion for isolating the palm area followed by then analyze the hand portion using the convex hull method. They also developed a virtual mouse by triggering all functions of a physical mouse with different customized gestures, and their proposed scheme achieved a recognition rate of more than 83% during inference time. Furthermore, in real-time scenario, a slight movement of the hand can lead to the jump of the virtual mouse cursor over the screen. So it is necessary to be concerned about the smoothness of the motion of the gesture-controlled mouse cursor. Literature survey has shown very few promising results about the smooth movement of the gesture-controlled mouse-cursor [16].

3 Proposed methodology

In this part, we have discussed different phases of our experiment. Firstly we have explained about pre-processing phase containing gesture detection, binary thresholding, contour portion selection, hand portion extraction, resizing and use of median filter for noise removal. Next the resized images are passed into six pre-trained CNN models (VGG16, VGG19, ResNet50, ResNet101, Inception-V1 and MobileNet-V1) for training them separately in order to obtain the final predicted gesture class. In the final part, we have extended our work by building a human-machine interface that identifies gesture labels as input commands. The entire block diagram of our proposed methodology is shown in Fig. 1.

3.1 Pre-processing phase

Image preprocessing is one of most significant and vital steps in order to improve the model performance. This phase comprises of some steps like gesture detection by background separation, binary thresholding of detected gesture portion, contour portion extraction, resizing of segmented images followed by using of median filter for noise removal. Next the resized images are fed into CNN models for classification task. All the steps are discussed in below and the entire pre-processing phase is shown in Fig. 2.

3.1.1 Gesture detection by background separation

Detection is a phase to identify an object within an image. During gesture detection, we have applied binary thresholding technique to segment between background and foreground portion, that makes background black and detected hand portion white in color. An example of detected hand portion in real-time scenario has been illustrated in Fig. 3.

3.1.2 Contour region selection and segmentation of hand portion

Contour region mainly indicates the outline/boundary of an object present in an image. To segment the hand region, we first need to get the contour region of the detected portion. Due to cluttered background or low-light situations, there might be multiple holes/contour portions in the detected portion. But the contour portion, with the largest area, is considered the hand region. Extraction of the hand region is accomplished by using the distance transformation method. In this method, first of all, we need to estimate the center of hand region (palm/hand center) [16,17]. According to this method, the pixel point in contour region, having maximum intensity is considered to be hand center. Palm radius is estimated by calculating the minimum distance between hand center and the point outside the contour region. Thus the hand region is separated from the arm based on wrist location. The whole diagram of contour portion selection to segmentation phase has been shown in Fig. 4.

3.1.3 Resizing of segmented images

Images resizing is essential in the preprocessing phase, as training with larger images consumes more time than smaller images. In our experiment, the segmented images have been resized into the resolution of (64×64) or (128×128) pixels before being fed into six transfer-learning-based CNN models for both feature extraction

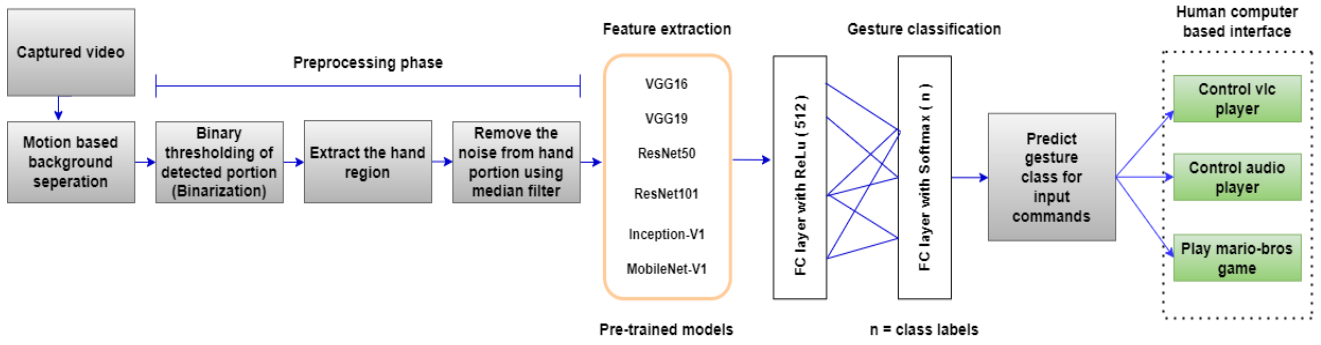


Fig. 1: Illustration of our proposed scheme.

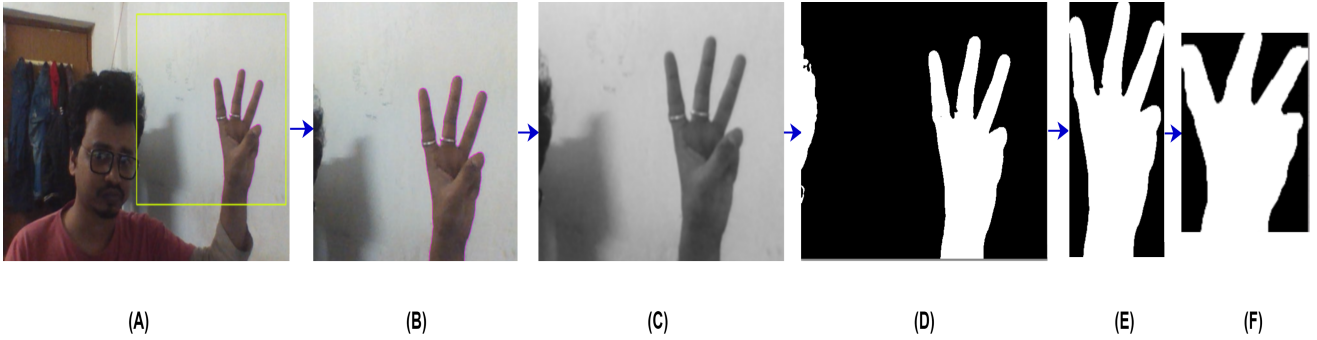


Fig. 2: The whole pre-processing phase of our proposed work (A) Input frame, (B) Gesture region detection, (C) conversion into gray scale, (D) Binary thresholding, (E) Extraction of hand region, (F) Applying of median filter for noise removal after resizing of segmented images.

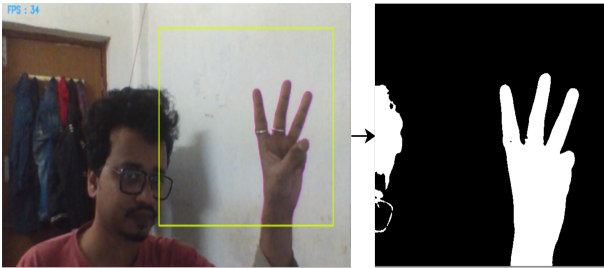


Fig. 3: Hand detection in real-time.

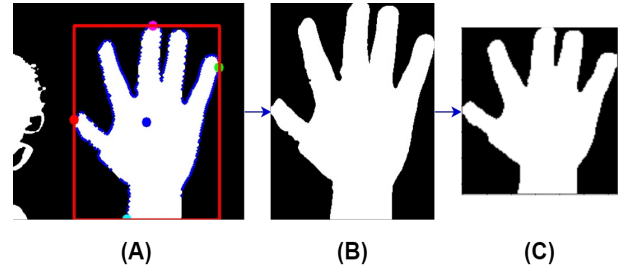


Fig. 4: Hand region segmentation procedure (A) Contour portion bounded by rectangle box, here blue point represents the hand center (B) segmented hand region, (C) resized segmented hand portion.

and classification task. Fig. 5, shows the segmented region and resizing of hand portion.

3.1.4 Noise removal using median filter

Median-filtering technique [18] is a noise removal technique that acts as lowpass filter in order to smooth and reduce noise from the images. In our experiment, this technique has been employed to remove the holes and unwanted parts from the segmented gesture portion after resizing phase.

3.2 Transfer-learning based CNN models

Building CNN models with millions of parameters from scratch is very time consuming with higher computation cost. So to overcome this issues, transfer learning method has been employed. It is a very effective method to use CNN models for solving image-classification related problems, where pre-trained models are reused to solve a new task. It is faster and requires less num-

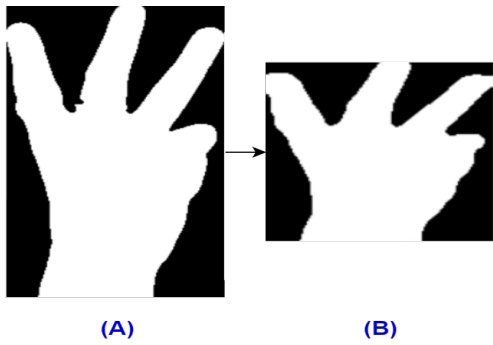


Fig. 5: (A) Segmented gesture region (B) resizing of segmented hand portion into aspect ratio of (64×64) .

ber of resources compared to CNN models built from scratch. In our work, some popular CNN models such as; VGG16 [19], VGG19 [19], ResNet50 [20], ResNet101, Inception-V1 [21] and MobileNet-V1 [22] have been explored followed by fine-tuning them using Adam optimizer on multi-class hand gesture datasets using transfer-learning approach. For obtaining the predicted output, we have replaced the final fully connected (FC) dense layer of each network with a new fully connected layer containing n number of nodes, where n denotes the number of classes present in three datasets. The details of these pre-trained architectures are illustrated in section Appendix A.

3.3 Use of Kalman filter

Kalman filtering [28] is one type of recursive predictive algorithm that provides the estimation of the state at time $(t-1)$ in a linear dynamic system in continuous manner. The equations for state space model is shown in Appendix section D.

In tracking mouse-cursor movement, first, we need to get the coordinates of the detected hand portion, followed by calculating the centroid. Centroid calculation is mandatory during hand movements because it is dynamic and changed with respect to time. In Fig. 6, the block diagram of Kalman filter based gesture tracking is illustrated.

4 Experiment

4.1 Datasets description

To validate the proposed scheme, several experiments are carried out using one self-constructed dataset (termed as Dataset-C) and two publicly available hand gesture image datasets [5, 23] (termed as Dataset-A, Dataset-B

respectively). Dataset-A comprises 20,000 gesture images of ten different gesture classes, such as: Fist, Fist move, Thumb, Index, Ok etc. The images of this dataset has been collected from ten different participants (five women and five men), where each class label has 200 images. The images are having dimension of (640×240) pixels. In Fig. 7, some samples of gesture images from Dataset-A and Dataset-B have been depicted. Dataset-B contains 16 gesture classes (such as, Fist move, Heavy, Ok, Five, Palm, Up, Index etc.) obtained from 25 participants (eight women and 17 men). In our experiment only static gesture images are considered, but all the gesture images have different pixel resolution.

We have also created our customized dataset (Dataset-C) containing 20,000 binary images collected by using the 16 megapixel USB webcam camera. This dataset contains 14 different gesture class labels collected by four participants (one woman and three men). Some samples of Dataset-C have been illustrated in Fig. 8. The details of the three datasets have been tabulated in Table 1.

Table 1: Dataset description

| Datasets | Number of people performed | No of gesture label | Total no of images |
|-----------|----------------------------|---------------------|--------------------|
| Dataset-A | 10 | 10 | 20,000 |
| Dataset-B | 25 | 16 | 86,986 |
| Dataset-C | 4 | 14 | 20,000 |

4.2 Dataset splitting

To perform all experiments, the datasets are randomly split into 80% for training and the remaining 20% for testing. Furthermore for validation purpose, training sets have been split into 75% for training and remaining 25% for validation. Now the percentage of training, validation and testing sets in the dataset will be 60%, 20% and 20% respectively. The training samples are used to fit the model, validation set is used to evaluate the performance on each model for hyper-parameter tuning or to select the best model out of different models. Remaining testing sets are used to evaluate the performance of our proposed model.

4.3 Experimental setup & details

All experiments have been carried out in Google Colab pro-environment, providing online cloud services with Tesla P100 Graphical Processing Unit (GPU), Central

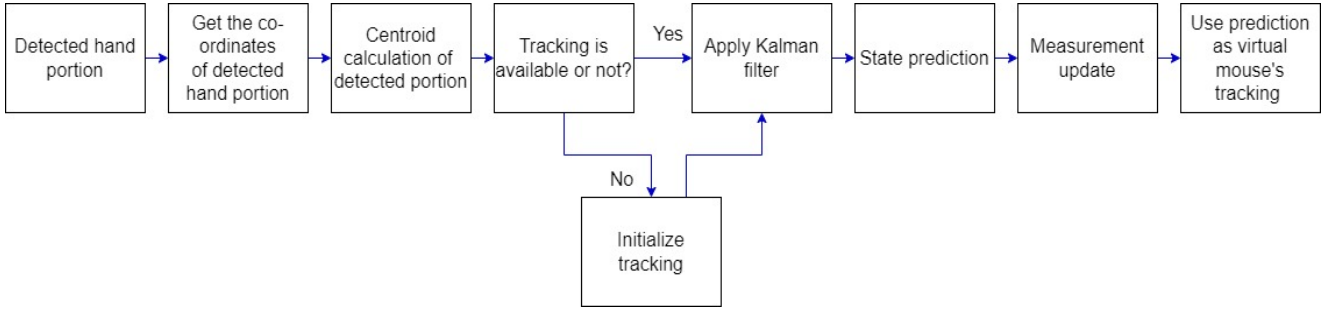


Fig. 6: Block diagram for Kalman filter based tracking.



Fig. 7: Samples images from Dataset-A and Dataset-B.

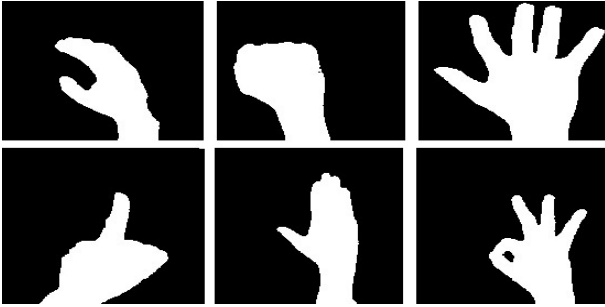


Fig. 8: Custom dataset samples.

Processing Unit (CPU), and 26 GB RAM. We have used Python programming language to train the deep learning models. We have divided our experiments into three parts: (1) ‘Experiment-1’, (2) ‘Experiment-2’, (3) ‘Experiment-3’ based on the n-class (number of gesture class labels) classification task.

‘Experiment-1’ and ‘Experiment-2’ have been carried out with Dataset-A and Dataset-B (previously mentioned in section 4.1) respectively, for solving both 10-class and 16-class classification problems. ‘Experiment-3’ has been performed to solve 14 gesture class classification problems by using Dataset-C (mentioned in section 4.1).

In the preprocessing phase of our experiment, firstly a binary thresholding operation has been conducted to

detect the gesture region by separating the background section. Then after the gesture detection phase, multiple contours regions are extracted from the resulting image, the region with having maximum area is considered as hand gesture portion. After getting the hand gesture images, they are resized into dimension of (64×64) and (128×128) pixels followed by median filtering [18] to exclude the noises and redundant parts from the resized gesture portions.

Six pre-trained models such as VGG16, VGG19, ResNet50, ResNet101, InceptionV1, and MobileNet-V1 are used for the feature extraction task, followed by adding of a dense layer (as output layer) containing nodes according to the number of classes present in Dataset-A, Dataset-B, and Dataset-C respectively to predict the final gesture class label. While training the models, the softmax activation function is used to find the probability values of the last output layers, where the maximum probability value decides the final gesture class label. Fine-tuning is done using the Adam optimizer, where the beta1 and beta2 are 0.9 and 0.99, respectively. We have set the initial learning rate as 0.0001 later; it has been multiplied by 10 after ten epochs. For all experiments, the batch size and the number of epochs/iterations are fixed as 64 and 30, respectively. The entire display of the hyper-parameter setting for the experiments are shown in Table 2.

Table 2: Display of Hyper-parameter settings.

| Used parameters | Values |
|----------------------|-------------------------------|
| Batch Size | 64 |
| Number of iterations | 30 |
| Learning rate | 0.0001, 0.001 after 10 epochs |
| Pooling size | (2×2) |
| Dropout | 0.2 |
| Optimizer | Adam |
| Error function | Categorical cross entropy |
| Activation function | ReLU, Softmax |

4.4 Results

In this portion, we have discussed over various results obtained from our three experiments (mentioned in section 4.3) performed on Dataset-A, Dataset-B and Dataset-C. The performances of our proposed work have been evaluated in terms of accuracy (%) and some evaluation metrics such as precision (PR), recall (RE) and F-score (harmonic mean of precision and recall) values obtained from the confusion matrix. These values are calculated by the indicators as TP (True Positive), FP (False Positive), FN (False Negative), and TN (True Negative) shown in Eqs. 1-3 (shown in Appendix B).

In our experiment, hand gesture classification accuracy is measured by the following formula:

$$\text{Accuracy} = \frac{\text{Number of correctly classified gesture samples}}{\text{Total number of gesture samples in testing sets}}$$

Experiment-1: This experiment solves ten-gesture class classification tasks based on six pre-trained CNN models over Dataset-A with a transfer learning approach. In Table 3, the transfer learning results of six pre-trained CNN models over Dataset-A for input size (64×64) and (128×128) have been reported. Here, it is noticed that the Inception-V1 model has earned maximum classification accuracy compared to other CNN classifiers. In Fig. 14, it is seen that the performance of the Inception-V1 model is better than the other models as it has reached lower values than the loss (training and validation) values of other pre-trained models. In Fig. 14, it is noticed that there is a lot of oscillation occurred in other models, but the Inception-V1 model appears to have less fluctuation as it is seen that both the training and validation curve has been converged. It is observed in Table 3 that the Inception-V1 model has a faster training time (sec) compared to other CNN models and provides better accuracy (%). The performance comparison of our proposed work (with the best-selected model, i.e., Inception-V1), with other state-of-the-art scheme on Dataset-A, has been illustrated in Table 4 in terms of class-wise accuracy values and the mean value. From comparative analysis (shown in Table 4), we can say that our proposed framework (detection + segmentation + median filter + Inception-V1 model) has outperformed the proposed scheme presented by [5] on Dataset-A in terms of accuracy results (class-wise accuracy). We have also conducted a statistical analysis to estimate the significant difference between the mean of the accuracy values by using one-sample t-test. The entire statistical testing is shown in Appendix Section C.

Experiment-2: This experiment has been performed on Dataset-B for solving 16-class problem. Here also, we have used six pre-trained CNN models with transfer-learning to obtain some fruitful results and compared the performance of these CNN models with other state-of-the-arts in terms of validation accuracy (%). The training time along with validation accuracy achieved by different classifiers are listed in Table 3. In Table 3, it is clearly noticed that the VGG16 model exhibits higher performance in terms of validation accuracy, but it has slower training time compared to the Inception-v1 model, so this model (Inception-V1) was further used to predict gesture class label in real-time scenario. In Fig. 15, it is observed that two graphs (termed as graph C and graph I) show the accuracy (training and validation) and loss (training and validation) plots for Inception-V1 model. These two plots exhibit less oscillations compared to other plots. So it can be said that Inception-V1 model has achieved a higher success.

Experiment-3: To show the effectiveness of our proposed scheme, we have performed this experiment on Dataset-C for solving the 14-gesture class classification task. Table 3 reports the validation accuracy results and training time obtained using six pre-trained CNN models after applying the transfer-learning approach. Table 3 shows that the Inception-V1 model has achieved the best result compared to other CNN models in terms of training time and validation accuracy. As shown in Fig. 16, both plots (accuracy and loss) C and I show fewer fluctuations, and both the curves (training and validation) have converged. So we can conclude that Inception-V1 has achieved superior results than other pre-trained CNN models and is further deployed for real-time HCI interface. The performance comparison of our proposed work with the other work proposed presented by [9] on Dataset-C has been tabulated in Table 5. The comparative analysis in Table 5 exhibits the superiority of our proposed scheme (segmentation, median filter, transfer-learning based CNN models) over other existing scheme [9] in terms of testing accuracy (%), precision (%), recall (%), and F-score (%).

4.5 Building of human-machine interface

Multimedia (example: audio, video) plays an essential part in our daily life with the advancement of technology. It is very interactive for every people in their everyday life in today's world. But the, physically impaired people find it challenging to interact with the systems. In this work, a human-machine interface has been presented to provide an idea for further improvements in controlling various desktop applications by using hand

Table 3: Comparison results among various pre-trained CNN models using transfer-learning approach on Dataset-A, Dataset-B and Dataset-C in terms of validation accuracy values.

| Dataset-A | | | | |
|-----------------------|---------------------|-------------------------|-------------------------|-------------------------|
| Input size: (64 × 64) | | | Input size: (128 × 128) | |
| Model name | Training time (sec) | Validation accuracy (%) | Training time (sec) | Validation accuracy (%) |
| VGG16 | 420 | 99.67 | 1290 | 99.60 |
| VGG19 | 510 | 99.65 | 1500 | 99.58 |
| Inception-V1 | 450 | 99.75 | 630 | 99.70 |
| ResNet50 | 660 | 99.60 | 1050 | 99.58 |
| ResNet101 | 870 | 99.70 | 1680 | 99.65 |
| MobileNet-V1 | 360 | 99.30 | 720 | 99.30 |

| Dataset-B | | | | |
|--------------|------|-------|------|-------|
| VGG16 | 1500 | 95.52 | 4650 | 95.17 |
| VGG19 | 1800 | 94.50 | 5100 | 95.46 |
| ResNet 50 | 2340 | 93.42 | 3450 | 93.39 |
| ResNet 101 | 3150 | 93.28 | 3750 | 93.44 |
| Inception V1 | 1400 | 93.57 | 2880 | 93.55 |
| MobileNet V1 | 1260 | 92.48 | 2700 | 92.20 |

| Dataset-C | | | | |
|--------------|-----|-------|------|-------|
| VGG16 | 600 | 99.25 | 1950 | 99.20 |
| VGG19 | 750 | 99.15 | 2400 | 99.20 |
| Inception-V1 | 240 | 99.30 | 800 | 99.25 |
| ResNet50 | 540 | 99.05 | 1500 | 99.00 |
| ResNet101 | 900 | 98.62 | 2400 | 98.50 |
| MobileNet-V1 | 240 | 99.10 | 780 | 99.08 |

Table 4: Comparative analysis of our proposed work (with Inception-V1 model) with existing approach on Dataset-A in terms of accuracy.

| Gesture class | Our work (using Inception-V1) | [5] Feature descriptor + SVM |
|---------------|----------------------------------|---------------------------------|
| Ok | 1 | 0.990 |
| Close | 0.990 | 1 |
| Palm | 1 | 1 |
| Thumb | 1 | 0.990 |
| Index | 1 | 1 |
| Fist | 1 | 0.990 |
| Palm move | 1 | 1 |
| Palm down | 1 | 1 |
| L | 1 | 0.990 |
| Fist move | 0.990 | 1 |
| Mean | 0.998 | 0.990 |

gesture commands, which will be beneficial for physically impaired persons. In our experiment, we have built an interface to control three applications (VLC media player, audio player, 2D-Marios Bros game) by using corresponding gesture commands after obtaining the predicted class label. We have also extended our work by developing a gesture-controlled virtual mouse and enhanced the smoothness of mouse-cursor movement by employing the Kalman filter.

Algorithm 1 Gesture-controlled human-machine interface

INPUT: Give predicted gesture as input commands after training by six pre-trained CNN models.

OUTPUT: Development of gesture-controlled HCI interface.

step 1: Choose the best CNN classifier after training, among the others in terms of accuracy and training time.

step 2: Get the predicted gesture class label.

for $k \leftarrow 1$ to C **do**, where $C \leftarrow$ number of applications.

Control each application according to the customized gesture-class (predicted) label.

end for

4.5.1 VLC-player control:

In our experiment, we have used the ‘vlc-ctrl’ [24] command-line interface to control various VLC player-related functions, such as play, pause, switch to next video, volume increase/decrease, quit. In our experiment, after obtaining the predicted gesture class label, the keyboard event of the keys is triggered using input gesture commands to control the VLC player. In Table 7, different controls of the VLC player have been tabulated according to various customized gesture labels. Demo of this gesture-controlled VLC-player has been illustrated in Fig. 9.

Real-time performance analysis of our proposed gesture-

Table 5: Performance comparison of our work with other state-of-the-art scheme on Dataset-C.

| Proposed scheme | Methods / models | Testing Accuracy (%) | Precision (%) | Recall (%) | F-score |
|--------------------|---|----------------------|---------------|------------|---------|
| Yingxin et al. [9] | Canny edge detection, CNN | 89.17 | 90.00 | 89.21 | 89.60 |
| Our work | Segmentation, median filter, VGG16 | 99.20 | 99.22 | 99.15 | 99.19 |
| Our work | Segmentation, median filter, VGG19 | 99.00 | 99.10 | 99.03 | 99.07 |
| Our work | Segmentation, median filter, Inception-V1 | 99.25 | 99.28 | 99.22 | 99.25 |
| Our study | Segmentation, median filter, ResNet50 | 98.35 | 99.20 | 99.25 | 99.28 |
| Our study | Segmentation, median filter, ResNet101 | 98.15 | 98.30 | 98.20 | 98.25 |
| Our Study | Segmentation, median filter, MobileNet-V1 | 98.85 | 98.95 | 98.80 | 98.88 |

command-based VLC-player control has been displayed in Table 6. For examples, gesture ‘Ok’ has been set to start the video. Similarly, gestures ‘Hang’ and ‘L’ for volume up and down respectively. The different controls of this application have been illustrated in Table 7. But due to the messy background, this application’s performance is sometimes hampered. We have also performed every control of the VLC player 10 times with the corresponding gesture-commands to obtain the proper detection rate (%) along with the response time. In Table 6, we have shown the number of hits and misses obtained by using our application, followed by calculating the gesture detection rate (%) and the average response time (in mili second).

$$\text{Gesture detection rate} = \frac{\text{Number of hits}}{\text{Total number of hits and misses}}$$

Response time = (time taken to detect gesture – time taken to perform any control of video / audio player with the corresponding gesture commands)

$$\text{Average response time} = \frac{\text{Total response time for each function}}{N}$$

Here N represents the total number of performance per each control, in our work $N=10$, as we have performed every control of VLC player and audio-player 10 times with the corresponding gesture commands.

4.5.2 Audio player control:

A summary for controlling different functions of audio-player using various gesture commands has been tabulated in Table 7, whereas Fig. 10 shows the demo of the gesture-controlled audio player. In our work, we have used the ‘audioplayer’ [25] python package and ‘play-erctl’ command-line library to use different features of the Spotify music player, such as playing a song, pausing, resuming, switching to the next song, and go to the previous music. We have executed every control of the Spotify player (such as: playing, pausing, resuming, etc.) ten times to obtain some valuable results. For instances shown in Table 7, gesture ‘Ok’ has been customized to play the song, similarly, ‘Five’ for pause,

‘Fist’ for resume, ‘Two’ for going to the next song, and ‘Three’ for a switch to the previous music. In Table 6, the performance of the gesture-controlled audio player (Spotify player) in real-time scenario, along with the number of hits, misses, and the average response time (in mili-seconds), has been depicted.

4.5.3 Super Mario-Bros game control

In this section, we have demonstrated the experimental details of the gesture-controlled super-Mario Bros game along with real-time performance analysis. Here we have used the OpenAI Gym environment and imported ‘gym – super – mario – bros’ [26] command-line interface to trigger different controls of this game based on various gesture commands. For example, the gesture ‘Ok’ has been set for the run of Mario character; similarly, gestures ‘Four’ and ‘Five’ have been customized for jumping to the left and right direction, respectively, and gesture ‘Two’ for hold/stay of the Mario. This game’s controls are tabulated in Table 7. One Demo of this game is shown in Fig. 11.

4.6 Building of virtual mouse

In order to make the interface more convenient, we have developed a virtual mouse, where main objective is to control various functions of a traditional mouse with the help of predicted gesture commands and a simple web-camera instead of physical mouse device. The main functions of a traditional mouse are click, right-click, double-click, drag, scroll wheel up/down and cursor movement. So in our work, we have mimicked different events of a physical mouse with seven corresponding gesture commands. For instances, the gestures ‘Two’ is set for right click, ‘Ok’ is for double click, ‘Index’ is for left click etc. Fig. 13 shows the schematic diagram of the virtual mouse and one demo of gesture-controlled virtual mouse is depicted in Fig. 12. The summary of different controls of virtual mouse according to customized gestures have been shown in Table 8. But still there is a problem regarding the smooth movement of the

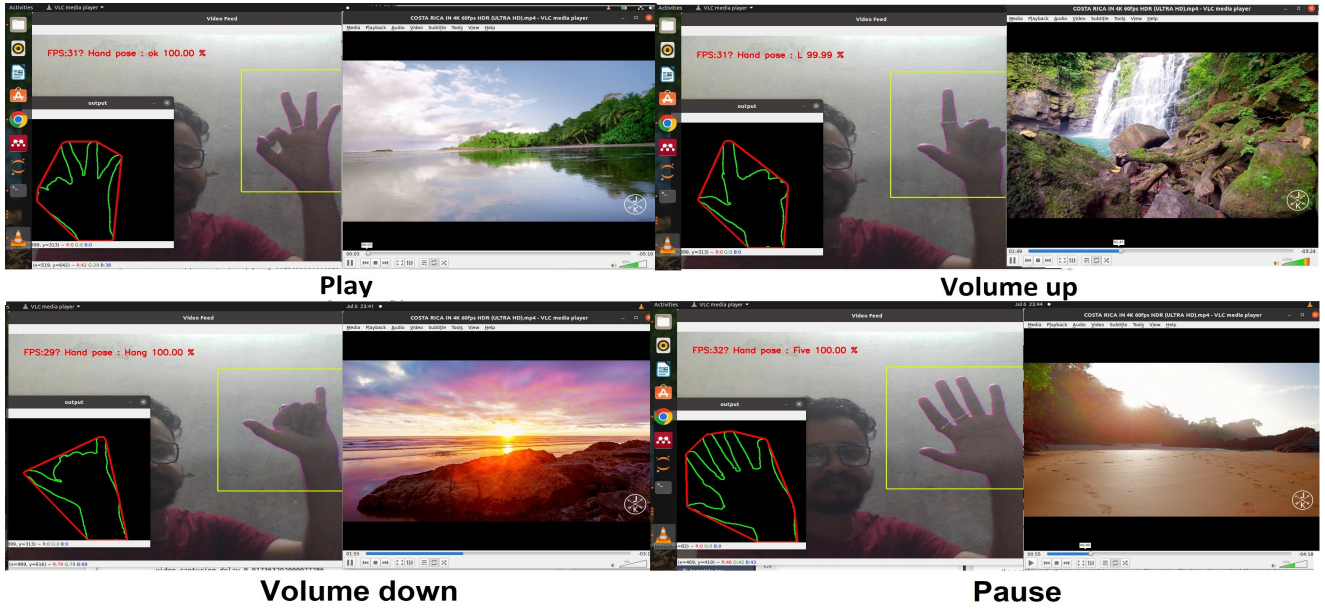


Fig. 9: VLC player control using gesture commands.

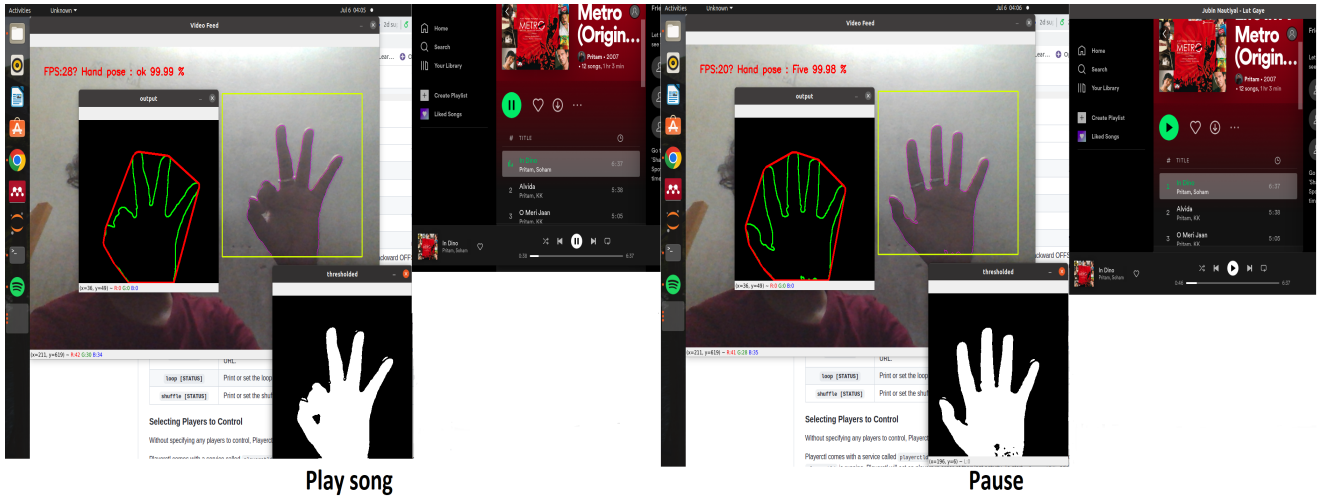


Fig. 10: Audio player (Spotify platform) control using gesture commands.

mouse cursor, for example, during slight hand movement, jumping of cursor from one position to another on the screen. We have also resolved this issue by applying the Kalman filtering [27]. In next section 3.3, we have shown the performance analysis of improved mouse cursor control using Kalman filter.

5 Discussions

An interactive HCI interface is suggested through a vision-based hand gesture classification system based on deep learning approach. We have performed several experiments on three datasets (details description in

section 4.1) to evaluate the potency of our proposed work.

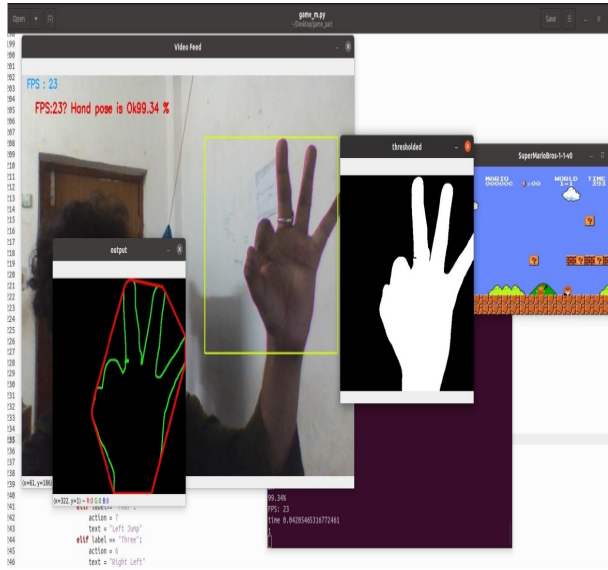
We have computed the performance of six pre-trained models using the transfer-learning approach for input size (64×64) and (128×128) . The results have been illustrated in Table 3. It is observed that the Inception-V1 model has outperformed the other CNN models due to having an Inception module, where (1×1) convolution was used for the dimension reduction purpose. Simultaneously, using this architecture reduces the computation cost, and training time becomes faster. So this CNN classifier is used for further deployment during real-time inference. It is also noticed in Table 3 that the time taken to train with the images of dimensions

Table 6: Real-time performance analysis of gesture-command based VLC and audio player control (10 times).

| Performance analysis of real-time gesture-command based VLC-player application (10 times) | | | | | |
|--|------------------------|----------------|------------------|--------------------|----------------------------|
| Action | Corresponding gestures | Number of hits | Number of misses | Detection rate (%) | Average Response time (ms) |
| Play | Ok | 10 | 0 | 100 | 0.35 |
| Volume Up | L | 8 | 2 | 80 | 0.83 |
| Volume down | Hang | 9 | 1 | 90 | 0.82 |
| Quit | Close | 10 | 0 | 100 | 0.38 |
| Go to next video | Two | 7 | 3 | 70 | 0.38 |
| Pause | Five | 9 | 1 | 90 | 0.40 |
| Performance analysis of audio-player (10 times) based on gesture command in real-time scenario | | | | | |
| Play | Ok | 10 | 0 | 100 | 0.30 |
| Pause | Five | 10 | 0 | 100 | 0.30 |
| Resume | Fist | 9 | 1 | 90 | 0.40 |
| Go to next song | Two | 8 | 2 | 80 | 0.35 |
| Go to previous song | Three | 7 | 3 | 70 | 0.35 |

Table 7: Desktop applications control by using different gesture commands.

| VLC player | | Audio player | | 2D Super-mario bros | |
|---------------|------------------|---------------|---------------------|---------------------|------------|
| Gesture label | Action | Gesture label | Action | Gesture label | Action |
| Ok | Play | Ok | Play | Ok | Run |
| L | Volume Up | Five | Pause | Five | Jump right |
| Hang | Volume down | Fist | Resume | Two | Hold/Stay |
| Close | Video quit | Two | Go to next song | Four | Jump left |
| Two | Go to next video | Three | Go to previous song | Thumb | Jump |
| Five | Pause | | | | |

**Fig. 11: 2D Mario-Bros game control using gesture commands.**

(64×64) pixel is less than the time taken to train the images of size (128×128). However, training with smaller images leads to a huge reduction in computational cost.

Table 8: Triggering of mouse events using customized gesture inputs.

| Gesture inputs | Action |
|----------------|------------------|
| Two | Right click |
| Ok | Double click |
| Index | Left click |
| Five | Pointer movement |
| Heavy | Scroll up |
| Hang | Scroll down |
| Palm | Drag |

So, during test-time also, the images are resized into the aspect ratio of (64×64) followed by being fed into the Inception-V1 model to provide the final gesture class label. Furthermore, the performance comparisons with the other state-of-the-art schemes have been depicted in Tables 4, 5. We have also extended our proposed scheme by building a real-time HCI interface and a gesture-controlled virtual mouse to control different applications (VLC player, audio player control, and 2D-Super-Marios game) using custom gesture commands. The real-time performance analysis for these applica-

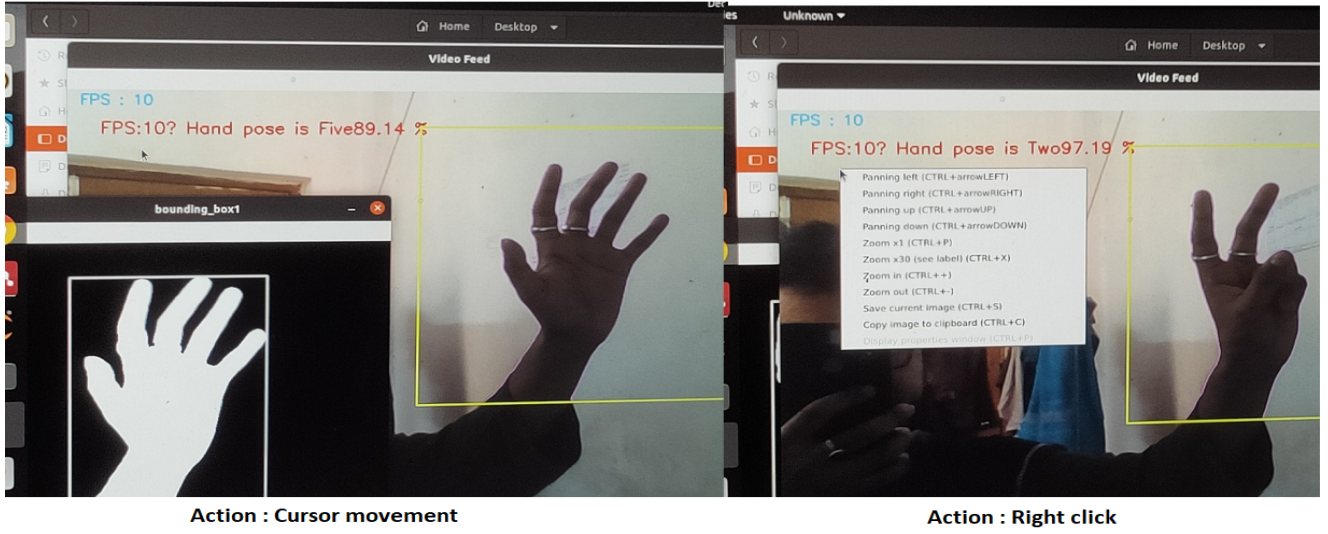


Fig. 12: Demo of gesture-controlled virtual mouse.

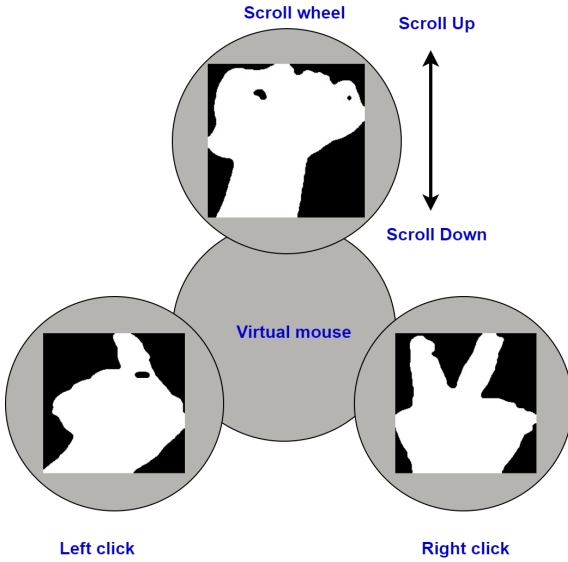


Fig. 13: Schematic diagram of virtual mouse.

tions has been shown in Table 6. The advantages of our proposed system are as follows.

- In the case of real-time gesture prediction, the system performs the classification task using the Inception-V1 model, which enables a faster training time with better accuracy.
- The average speed of this system is 35 fps (frames per second), which meets the perfect requirements for real-time apps controlling.
- This HCI interface is highly beneficial for interacting with desktop applications without touching any mouse or keyboard in a real-time scenario. So this

system can be a preferred choice for the older or physically disabled people.

Despite the advantages mentioned above of our proposed system, this system encounters some drawbacks during real-time gesture prediction in the cluttered background because it creates multiple contour regions leading to the segmentation error (failed to segment the gesture portion). Illumination variation and distance issues are also challenges in our proposed system. Another project issue is controlling the higher fps applications, as the average speed of our proposed scheme is 35 fps. Furthermore, using the Kalman filter delays the virtual mouse's performance a bit slow in a real-time scenario. We will explore some effective object detection techniques, such as Faster RCNN [29], EfficientDet [30], etc., to detect the gestures in the messy background and will bring some modifications to the Kalman filtering algorithm to avoid the time delay appears during the real-time performance.

6 Conclusion

In this paper, one interactive HCI through a hand gesture recognition system has been depicted. Our proposed framework consists of a set of stages, such as (1) binary thresholding technique to detect the gesture portion, (2) gesture segmentation, (3) application of the median filter on the resized segmented portions to remove the noise, (4) fed the resized images into six pre-trained models for training, (5) choose the best model among six classifiers for deployment task, (6) build a real-time HCI to control three desktop applications along with the development of the virtual mouse

using gesture-commands. Two publicly and one custom datasets have been considered to validate our proposed approach. We have compared the performance of six pre-trained CNN architectures using the transfer-learning method. The results exhibit that the Inception-V1 model has achieved better results on Dataset-A, Dataset-B, and Dataset-C in terms of training time and validation accuracy (%). The comparative analysis with other proposed schemes also shows that the Inception-V1 model exhibited superior results and was chosen for the real-time gesture classification task for faster training time (sec) and also better accuracy (%). Moreover, we have applied the Kalman filter to make the motion of the gesture-controlled mouse cursor smoother. In our future work, we will build a robust and efficient HCI interface by connecting other modalities, such as eye-gaze tracking, facial expression, etc., to make the system more convenient and user-friendly.

References

1. V. Bereznoy, D. Popov, I. Afanasyev, N. Mavridis, The hand-gesture-based control interface with wearable glove system., in: ICINCO (2), 2018, pp. 458–465.
2. K. S. Abhishek, L. C. F. Qubeley, D. Ho, Glove-based hand gesture recognition sign language translator using capacitive touch sensor, in: 2016 IEEE International Conference on Electron Devices and Solid-State Circuits (EDSSC), IEEE, 2016, pp. 334–337.
3. C.-J. Liao, S.-F. Su, M.-C. Chen, Vision-based hand gesture recognition system for a dynamic and complicated environment, in: 2015 IEEE International Conference on Systems, Man, and Cybernetics, 2015, pp. 2891–2895. doi:10.1109/SMC.2015.503.
4. F. Al Farid, N. Hashim, J. Abdullah, M. R. Bhuiyan, W. N. Shahida Mohd Isa, J. Uddin, M. A. Haque, M. N. Husen, A structured and methodological review on vision-based hand gesture recognition system, Journal of Imaging 8 (6) (2022) 153.
5. T. Mantecón, C. R. del Blanco, F. Jaureguizar, N. García, Hand gesture recognition using infrared imagery provided by leap motion controller, in: International Conference on Advanced Concepts for Intelligent Vision Systems, Springer, 2016, pp. 47–57.
6. D.-Y. Huang, W.-C. Hu, S.-H. Chang, Gabor filter-based hand-pose angle estimation for hand gesture recognition under varying illumination, Expert Systems with Applications 38 (5) (2011) 6031–6042.
7. J. Singha, A. Roy, R. H. Laskar, Dynamic hand gesture recognition using vision-based approach for human-computer interaction, Neural Computing and Applications 29 (4) (2018) 1129–1141.
8. Z. Yang, Y. Li, W. Chen, Y. Zheng, Dynamic hand gesture recognition using hidden markov models, in: 2012 7th International Conference on Computer Science & Education (ICCSE), IEEE, 2012, pp. 360–365.
9. X. Yingxin, L. Jinghua, W. Lichun, K. Dehui, A robust hand gesture recognition method via convolutional neural network, in: 2016 6th international conference on digital home (ICDH), IEEE, 2016, pp. 64–67.
10. O. K. Oyedotun, A. Khashman, Deep learning in vision-based static hand gesture recognition, Neural Computing and Applications 28 (12) (2017) 3941–3951.
11. W. Fang, Y. Ding, F. Zhang, J. Sheng, Gesture recognition based on cnn and dcgan for calculation and text output, IEEE access 7 (2019) 28230–28237.
12. V. Adithya, R. Rajesh, A deep convolutional neural network approach for static hand gesture recognition, Procedia Computer Science 171 (2020) 2353–2361.
13. A. Sen, T. K. Mishra, R. Dash, A novel hand gesture detection and recognition system based on ensemble-based convolutional neural network, Multimedia Tools and Applications (2022) 1–24.
14. K. H. Shibly, S. K. Dey, M. A. Islam, S. I. Showrav, Design and development of hand gesture based virtual mouse, in: 2019 1st International Conference on Advances in Science, Engineering and Robotics Technology (ICAS-ERT), IEEE, 2019, pp. 1–5.
15. T.-H. Tsai, C.-C. Huang, K.-L. Zhang, Design of hand gesture recognition system for human-computer interaction, Multimedia tools and applications 79 (9) (2020) 5989–6007.
16. P. Xu, A real-time hand gesture recognition and human-computer interaction system, arXiv preprint arXiv:1704.07296.

17. Z.-h. Chen, J.-T. Kim, J. Liang, J. Zhang, Y.-B. Yuan, Real-time hand gesture recognition using finger segmentation, *The Scientific World Journal* 2014.
18. G. George, R. M. Oommen, S. Shelly, S. S. Philipose, A. M. Varghese, A survey on various median filtering techniques for removal of impulse noise from digital image, in: 2018 conference on emerging devices and smart systems (ICEDSS), IEEE, 2018, pp. 235–238.
19. K. Simonyan, A. Zisserman, Very deep convolutional networks for large-scale image recognition, *arXiv preprint arXiv:1409.1556*.
20. K. He, X. Zhang, S. Ren, J. Sun, Deep residual learning for image recognition, in: *Proceedings of the IEEE conference on computer vision and pattern recognition*, 2016, pp. 770–778.
21. C. Szegedy, W. Liu, Y. Jia, P. Sermanet, S. Reed, D. Anguelov, D. Erhan, V. Vanhoucke, A. Rabinovich, Going deeper with convolutions, in: *Proceedings of the IEEE conference on computer vision and pattern recognition*, 2015, pp. 1–9.
22. A. G. Howard, M. Zhu, B. Chen, D. Kalenichenko, W. Wang, T. Weyand, M. Andreetto, H. Adam, Mobilenets: Efficient convolutional neural networks for mobile vision applications, *arXiv preprint arXiv:1704.04861*.
23. T. Mantecón, C. R. Del-Blanco, F. Jaureguizar, N. García, A real-time gesture recognition system using near-infrared imagery, *PloS one* 14 (10) (2019) e0223320.
24. *Vlc-ctrl*.
URL <https://pypi.org/project/vlc-ctrl/>
25. *Audioplayer*.
URL <https://pypi.org/project/audioplayer/>
26. C. Kauten, Super Mario Bros for OpenAI Gym, *GitHub* (2018).
27. M. S. M. Asaari, S. A. Suandi, Hand gesture tracking system using adaptive kalman filter, in: 2010 10th International Conference on Intelligent Systems Design and Applications, IEEE, 2010, pp. 166–171.
28. Y. Kim, H. Bang, *Introduction to kalman filter and its applications*, in: F. Govaers (Ed.), *Introduction and Implementations of the Kalman Filter*, IntechOpen, Rijeka, 2018, Ch. 2. doi:10.5772/intechopen.80600.
URL <https://doi.org/10.5772/intechopen.80600>
29. S. Ren, K. He, R. Girshick, J. Sun, Faster r-cnn: Towards real-time object detection with region proposal networks, *Advances in neural information processing systems* 28.
30. M. Tan, R. Pang, Q. V. Le, Efficientdet: Scalable and efficient object detection, in: *Proceedings of the IEEE/CVF conference on computer vision and pattern recognition*, 2020, pp. 10781–10790.
31. J. Deng, W. Dong, R. Socher, L.-J. Li, K. Li, L. Fei-Fei, Imagenet: A large-scale hierarchical image database, in: 2009 IEEE conference on computer vision and pattern recognition, Ieee, 2009, pp. 248–255.

A Appendix

A.1 VGG16

VGG16 architecture is an one type of variant of VGGNet [19] model, consisting of 13 convolutional layers with kernel sizes of (3×3) and Relu activation function. Each convolution layer is pursued by max-pooling layer with filter size (2×2) . Finally the FC layer is added with softmax activation function to produce the final output class label. In this architecture, the depth of network is increased by adding more

convolution and max-pooling layers. This network is trained on large-scale ImageNet [31] dataset, ImageNet dataset consists of millions of images and having more than 20,000 class labels developed for large scale visual recognition challenge. VGG16 has reported test accuracy of 92.7% in the ILSVRC-2012 challenge.

A.2 VGG19

VGG19 is also a variant of VGGNet network [19], it comprises 16 convolutional layers and three dense layers with kernel /filter size of (3×3) and then the max-pooling layer is used with filter size (2×2) . This architecture is pursued by the final FC layer with softmax function to deliver the predicted class label. This model has achieved second rank in ILSVRC-2014 challenge after being trained on ImageNet [31] dataset. This model has an input size of (224×224) .

A.3 Inception-V1

Inception-V1 or GoogleNet [21] is a powerful CNN architecture with having 22 layers built on the inception module. In this module, the architecture is limited by three independent filters such as (1×1) , (3×3) and (5×5) . Here in this architecture, (1×1) filter is used before (3×3) , (5×5) convolutional filters for dimension reduction purpose. This module also includes one max-pooling layer with pool size (3×3) . In this module the outputs by using convolutional layers such as (1×1) , (3×3) and (5×5) are concatenated and form the inputs for next layer. The last part follows the FC layer with a softmax function to produce the final predicted output. This input of this model is (224×224) . This architecture is trained with ImageNet [31] dataset and has reported top-5 error of 6.67% in ILSVRC-2014 challenge.

A.4 ResNet50:

Residual neural network [20] was developed by Microsoft research, This model consists of 50 layers, where 50 stands total number of deep layers, containing 48 convolutional layers, one max-pooling. Finally global average pool layer is connected to the top of the final residual block, which is pursued by the dense layer with softmax activation to generate the final output class. This network has input size of (224×224) . The backbone of this architecture is based on residual block. In the case of residual block, the output of one layer is added to a deeper layer in the block, which is also called skip connections or shortcuts. This architecture also reduces the vanishing and exploding gradient problems during training. ResNet50 architecture was trained on the ImageNet dataset [31] and has achieved a good results in ILSVRC-2014 challenge with an error of 3.57%.

A.5 ResNet101:

ResNet101 model consists of 101 deep layers. Like ResNet50, this architecture is also based on the residual building block. In our experiment, we have loaded the pre-trained version of this architecture, trained on ImageNet dataset [31] that comprises millions of images. This model's default input image size is (224×224) .

A.6 MobileNet-V1:

MobileNet-V1 architecture [22] is a light-weighted model which is mainly based on streamline architecture that uses depth-wise separable convolution and point-wise convolution (1×1 convolution). MobileNet architecture consists of 28 layers, where each depth-wise separable convolution layer includes both depth-wise and point-wise convolution. This architecture is better known for its small model size and lower computation cost. In this model, all layers are followed by batch normalization and ReLU activation function, then fed into the final FC layer for classification with softmax activation function to get the probability values of the final output layers hence the maximum probability value decides the final class label. The network also has the input image size of (224×224).

B Appendix

$$PR = \frac{TP}{TP + FP} \quad (1)$$

$$RE = \frac{TP}{TP + FN} \quad (2)$$

$$F - score = \frac{2 \times PR \times RE}{PR + RE} \quad (3)$$

C Appendix

C.1 Statistical hypothesis testing

We have also performed a statistical analysis in order to check statistical significance of our model. In Experiment-1 4.4, we have conducted one sample t -test with the help of IBM SPSS statistical analysis tool. In case of null hypothesis, we have to assume that our model is not statistically significant.

To obtain the value of t , the following formula is used:

$$t = \frac{(\bar{X} - \mu)}{\frac{SD}{\sqrt{k}}}$$

Table 9: One sample statistics.

| Number of samples | Mean | Standard deviation | Standard error mean |
|-------------------|---------|--------------------|---------------------|
| 10 | 99.8300 | 0.2907 | 0.0919 |

Where \bar{X} is the mean of samples.

μ the test value.

SD sample standard deviation.

k size of samples.

To get the value of \bar{X} , firstly, we have used the ten-fold-cross-validation strategy using Dataset-1, and have calculated the fold-wise accuracy followed by computing the average (considered as sample mean) of these accuracy values with the Inception-V1 (best-selected model for Experiment-1 4.4) model.

Table 9 shows that the sample mean (\bar{X}), sample size (k), test value (μ), and the standard deviation (SD) are 99.83, 10,

99, and 0.2907, respectively, and the entire statistical analysis of one-sample t -test has been demonstrated in Table 10.

The results in Table 10 exhibit that p -value < 0.001 . Here p -value is used for hypothesis testing to determine whether there is evidence to reject the null hypothesis.

If $p < \alpha$ where, α (confidence level) = 0.05, then null hypothesis is rejected.

In Table 10, it is observed that p -value is very less than α , so the null hypothesis is rejected, and we can say that there is a statistically significant difference in the mean of the accuracy values.

D Appendix

$$x_{t+1} = A_t * x_t + B_t * u_t + \epsilon_t \quad (4)$$

$$z_t = H_t * x_t + \beta_t \quad (5)$$

where x_t , A_t , B_t , u_t , ϵ_t , z_t , β_t , H_t are the current state vector, the control input, noise the measured state vector, the state transition model, the control model respectively.

This filter comprises of two stages, (1) state prediction, (2) measurement update. In the first phase, it estimates the state in the system and in the second phase, estimated state is corrected resulting the error minimization in the covariance matrix.

Table 10: One-sample T-test result.

| One-sample Test | | | | | | |
|------------------------|----|--------------|-------------|-----------------|--|-------|
| | | Significance | | Test value= 99 | 95% Confidence interval of the difference | |
| t | df | One-Sided p | Two-Sided p | Mean Difference | Lower | Upper |
| 9.026 | 9 | <0.001 | <0.001 | 0.8300 | 0.6219 | 1.038 |

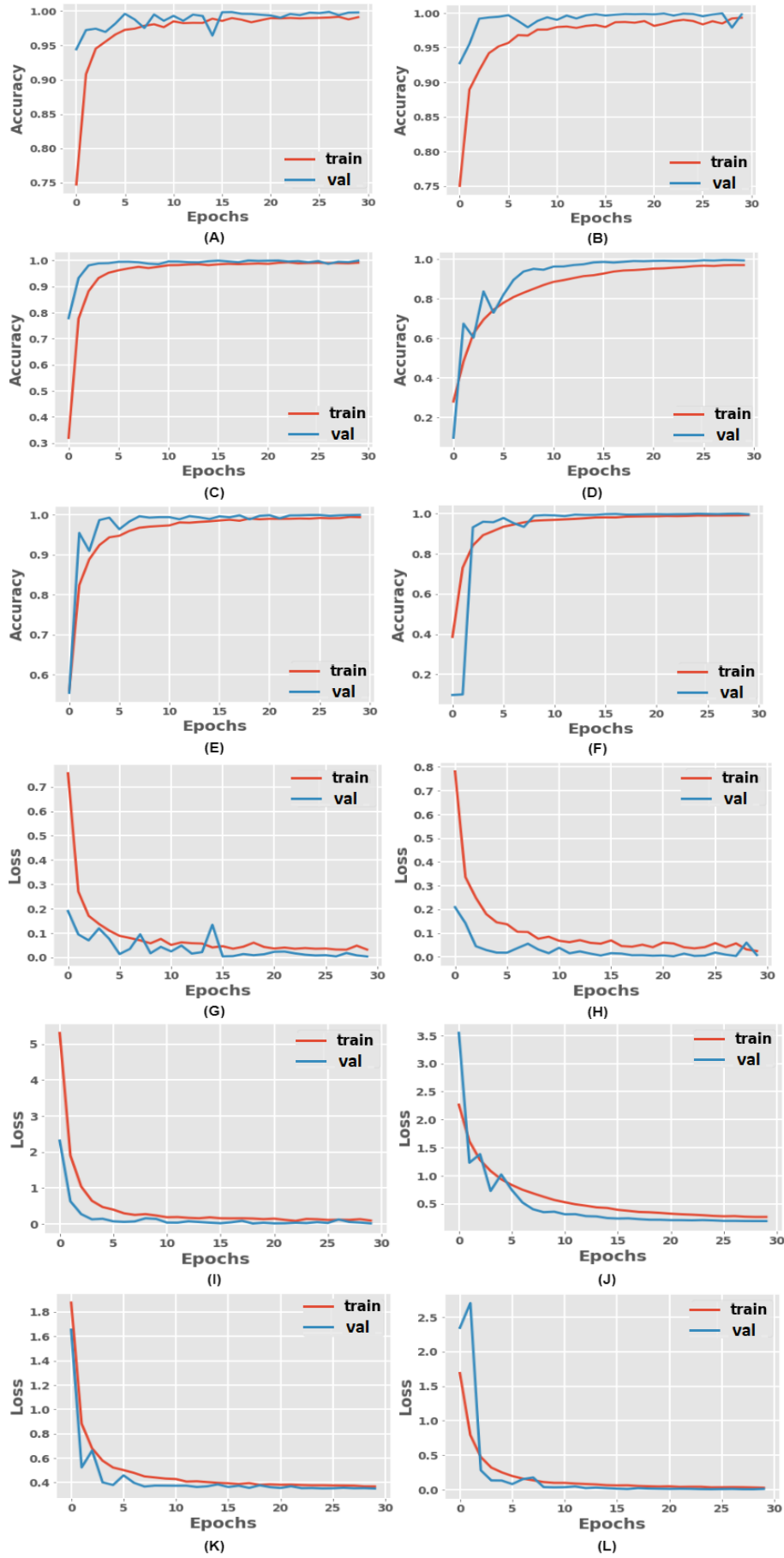


Fig. 14: Accuracy (training and validation) versus and loss (training and validation) plots for each model: Graphs A to F show the accuracy (training and validation) plots of each CNN model (VGG16, VGG19, Inception-V1, ResNet50, ResNet101, and MobileNet-V1 respectively). G to L show the loss plot for each model for Dataset-A.

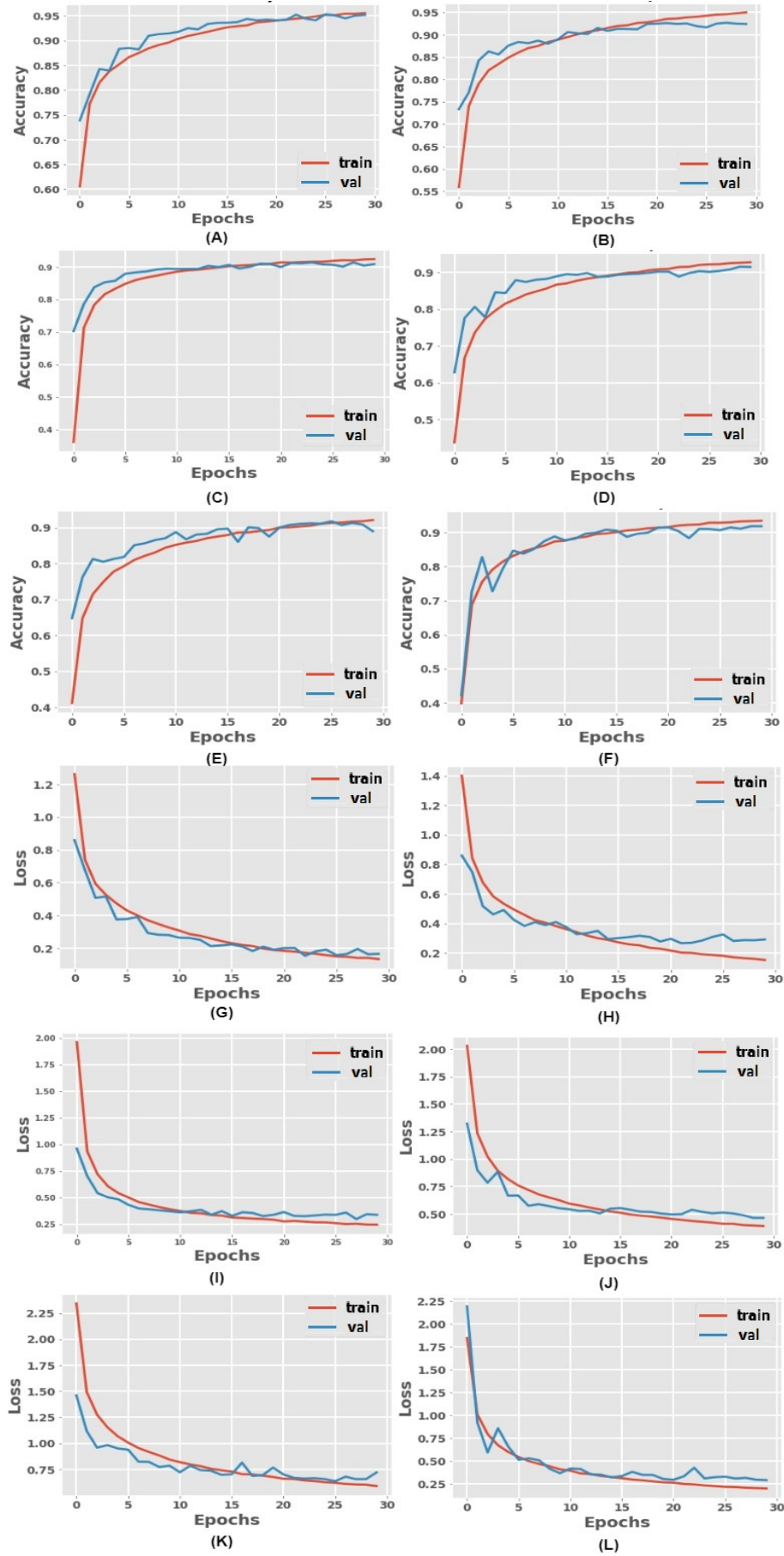


Fig. 15: Number of iterations versus accuracy (training and validation) and loss (training and validation) plots for each model: Graphs A to F show the accuracy (training and validation) plots of each CNN model (VGG16, VGG19, Inception-V1, ResNet50, ResNet101, and MobileNet-V1 respectively). G to L show the loss plot for each model for Dataset-B.

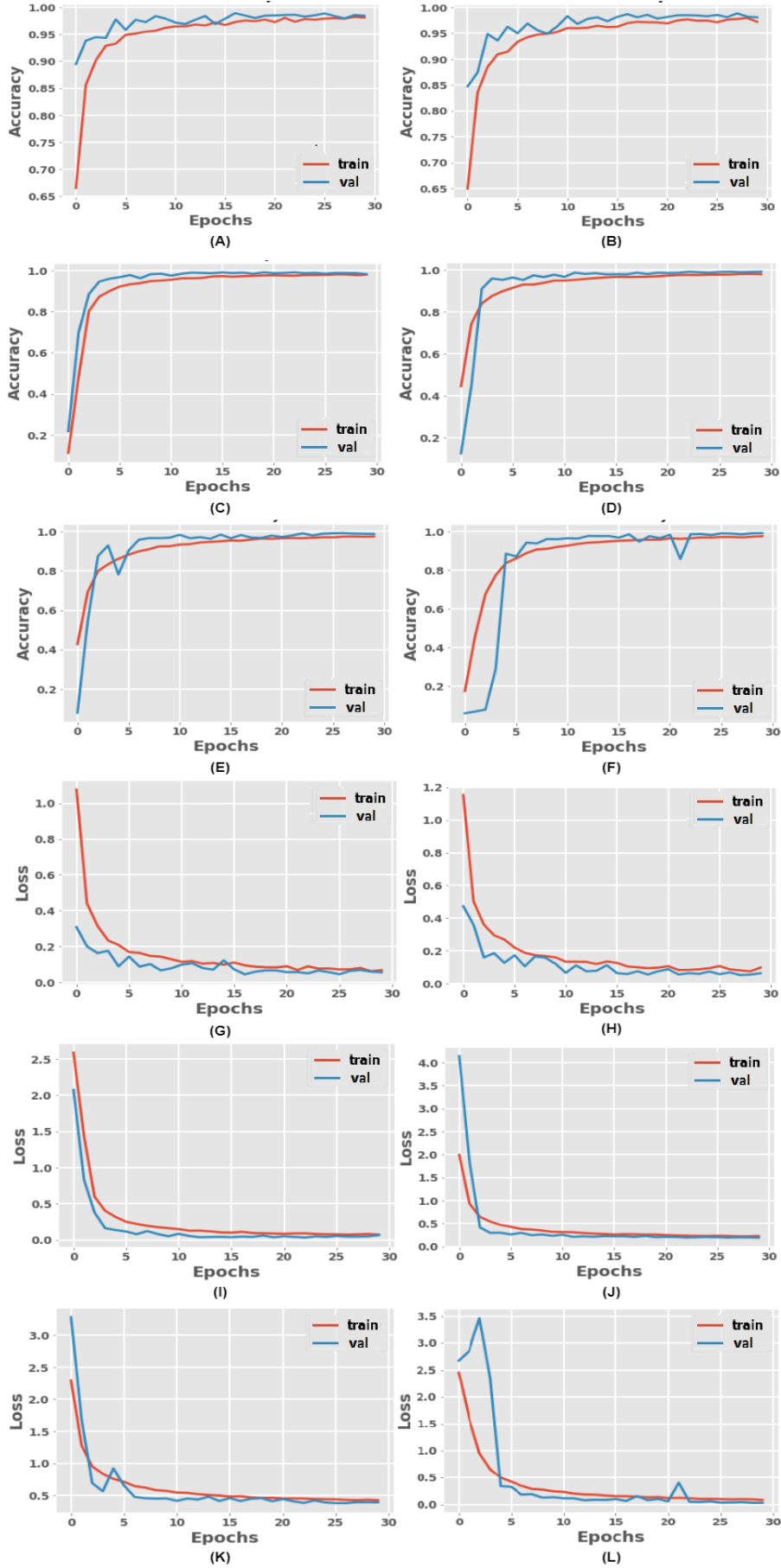


Fig. 16: Number of iterations versus accuracy (training and validation) and loss (training and validation) plots for each model: Graphs A to F show the accuracy (training and validation) plots of each CNN model (VGG16, VGG19, Inception-V1, ResNet50, ResNet101, and MobileNet-V1 respectively). G to L show the loss plot for each model for Dataset-C.